

Localization of collisionally inhomogeneous condensates in a bichromatic optical lattice

Yongshan Cheng^{1,2*} and S. K. Adhikari^{1†}

¹*Instituto de Física Teórica, UNESP - Universidade Estadual Paulista, 01.140-070 São Paulo, São Paulo, Brazil*

²*Department of Physics, Hubei Normal University, Huangshi 435002, People's Republic of China*

By direct numerical simulation and variational solution of the Gross-Pitaevskii equation, we studied the stationary and dynamic characteristics of a cigar-shaped, localized, collisionally inhomogeneous Bose-Einstein condensate trapped in a one-dimensional bichromatic quasi-periodic optical-lattice potential, as used in a recent experiment on the localization of a Bose-Einstein condensate [Roati *et al.*, *Nature* (London) **453**, 895 (2008)]. The effective potential characterizing the spatially modulated nonlinearity is obtained. It is found that the collisional inhomogeneity has influence not only on the central region but also on the tail of the Bose-Einstein condensate. The influence depends on the sign and value of the spatially modulated nonlinearity coefficient. We also demonstrate the stability of the stationary localized state by performing a standard linear stability analysis. Where possible, the numerical results are shown to be in good agreement with the variational results.

PACS numbers: 03.75.Lm, 67.85.Hj, 71.23.An

I. INTRODUCTION

Since Anderson predicted a localization of noninteracting electron wave in solids with a disorder potential fifty years ago [1], the Anderson localization has been observed and studied extensively in optics [2] and acoustics [3] and in Bose-Einstein condensates (BEC). In the study of Anderson localization in a BEC, disorder laser speckles [4] and quasi-periodic optical lattices (OL) [5] have been used. Random speckle potentials are produced when light is reflected by a rough surface or transmitted by a diffusive medium [6]. Billy *et al.* [4] observed the exponential tail of the spatial density distribution when a ⁸⁷Rb BEC was released into a one-dimensional (1D) waveguide in the presence of a controlled disorder created by a weak laser speckle. A bichromatic OL is realized by a primary lattice perturbed by a weak secondary lattice with incommensurate wavelength [7], and this system corresponds to an experimental realization of the Harper [8] or Aubry-André model [9]. Roati *et al.* [5] studied the localization of a noninteracting ³⁹K BEC in a bichromatic OL. There have been many theoretical studies of localization using the numerical solution of the Gross-Pitaevskii (GP) equation [10] as well as using the Bose-Hubbard model [11] in addition to the experimental studies under different conditions on disorder [12]. There have been studies of localization in two- and three-dimensions [13] and of the destruction of localization with the increase of nonlinear repulsion [14, 15].

A Feshbach resonance (FR) driven by a magnetic [16] or optical [17] field allows one to vary the atomic interaction of a BEC in a controlled fashion [18], thus creating a noninteracting as well as a weakly interacting BEC for the study of Anderson localization. Fedichev *et al.* [19] predicted that the spatial variation of the laser

field intensity by proper choice of the resonance detuning can lead to a spatial dependence of the atomic interaction, creating the so-called “collisionally inhomogeneous” BECs. The theoretical prediction has been demonstrated experimentally by Theis *et al.* with the ⁸⁷Rb BEC [17]. Sakaguchi and Malomed studied the formation of solitons in such BECs [20]. There have been studies of matter-wave bright and dark solitons of the cubic-quintic nonlinear Schrödinger equation with time- and space-dependent nonlinearities [21] in a collisionally inhomogeneous environment, and of dynamical effects of a bright soliton BEC with local and smooth space variations of the two-body atomic scattering length [22]. There have been studies about how to introduce a space dependence in the nonlinear interaction of the BEC in a controlled way [23]. There have also been studies of soliton oscillations [24] and dynamical trapping and transport [25] in collisionally inhomogeneous BECs.

Here we combine the two interesting settings, namely, the bichromatic OL and a collisionally inhomogeneous BEC (with a spatially modulated nonlinearity), to study the statics and dynamics of a localized BEC in this set up. We assume that the spatial dependence of the nonlinearity, induced by the external magnetic field of the OL, has the same form as the bichromatic OL, i.e., the nonlinear coefficient in the GP equation is proportional to the OL intensity [20, 26]. We study the effects of the spatially modulated nonlinearity on the shape of the density envelope, and the stability of the stationary localized states. The numerical results are shown to be in good agreement with the variational results, where applicable. On the other hand, the tail region of the stationary localized states is examined, where we find exponential decay in space indicating localization in a weak disorder potential. We study the location oscillation (oscillation of the center) and breathing oscillation of the localized states, induced by appropriate perturbation, employing numerical simulation of the GP equation.

In Sec. II we present a brief account of the 1D GP equation and the bichromatic OL potential used in our

*yong.shan@163.com

†adhikari@ift.unesp.br; URL: www.ift.unesp.br/users/adhikari

study, and a time-dependent variational analysis of the GP equation under appropriate conditions. We obtain a set of coupled evolution equations for the parameters of the localized state. The effective potential characterizing the spatially modulated nonlinearity is also described. In Sec. III we investigate the effects of the spatially modulated nonlinearity on the central and tail regions of a stationary localized BEC by a numerical solution of the GP equation using the split-step Fourier spectral method. For the central region, we demonstrate the stability of the localized states by performing a standard linear stability analysis. In Sec. IV the oscillation dynamics of a collisionally inhomogeneous BEC in a bichromatic OL is studied numerically. In Sec. V we present a brief discussion and concluding remarks.

II. ANALYTICAL CONSIDERATION OF LOCALIZATION

We consider a cigar-shaped quasi 1D BEC with inhomogeneous atomic interaction described by wave function $u(x, t)$ satisfying the following dimensionless 1D GP equation [27, 28]

$$i\frac{\partial u}{\partial t} = -\frac{1}{2}\frac{\partial^2 u}{\partial x^2} + g(x)|u|^2u + V(x)u, \quad (1)$$

with normalization $\int_{-\infty}^{\infty} |u|^2 dx = 1$. The space variable x , time t , and energy are expressed in transverse harmonic oscillator units $a_{\perp} = \sqrt{\hbar/(m\omega)}$, ω^{-1} and $\hbar\omega$, where m is the mass of an atom and ω is the angular frequency of the transverse trap. As in the experiment of Roati *et al.* [5], the potential $V(x)$ is taken to be a bichromatic OL of incommensurate wave lengths:

$$V(x) = \sum_{l=1}^2 A_l \sin^2(k_l x), \quad (2)$$

with $A_l = 2\pi^2 s_l / \lambda_l^2$, ($l = 1, 2$), where λ_l 's are the wave-lengths of the OL potentials, s_l 's are their intensities, and $k_l = 2\pi/\lambda_l$ the corresponding wave numbers. In this investigation, we take the incommensurate ratio of the two components [29] $k_2/k_1 = (\sqrt{5}-1)/2 \approx 0.618033989\dots$. In the actual experiment of Roati *et al.* [5], however, the parameter is $k_2/k_1 = 1.1972\dots$. Without losing generality, we further take $\lambda_1 = 10$, and $s_1 = 10$, $s_2 = 0.3s_1$ which is roughly the same ratio s_2/s_1 as in the experiment of Roati *et al.* [5].

By means of the FR technique controlled by properly designed configurations of external optical fields [20, 26], the spatial variation of laser field intensity $I(x)$ produces the spatial variation of the atomic scattering length. As the potential $V(x)$ is also proportional to laser field intensity, it is reasonable to assume the spatial-dependence of the atomic scattering length is similar to $V(x)$. Then, the atomic scattering length can be given as $a_s = a_{s0} + cV(x)$; here $V(x)$ is the same as Eq. (2), a_{s0} is scattering length

of the corresponding collisionally homogeneous system, and c is a constant coefficient related to the optical intensity and may be either positive or negative. Thus, the nonlinear coefficient $g(x)$ in Eq. (1) has a spatial dependence of the form,

$$g(x) = \varepsilon_0 + \varepsilon \sum_{l=1}^2 A_l \sin^2(k_l x). \quad (3)$$

The nonlinearity ε_0 is given by [27] $\varepsilon_0 = 2a_{s0}N/a_{\perp}$ with N the number of atoms, and $\varepsilon = 2cN/a_{\perp}$ is the spatially modulated nonlinearity coefficient. Because the intensity-independent nonlinear coefficient ε_0 may be altered independently of the other parameters [18], in order to focus our attention on the effect of the spatially modulated nonlinearity on the localization of the BEC, we let $\varepsilon_0 = 0$ in the following.

Usually, the BEC localized states formed on a bichromatic lattice may occupy many sites of OL potential [5, 30]. For certain values of the parameters, however, potential (2) leads to localized states confined practically to a single site of the OL potential. When this happens, a variational approach for solving the GP equation is useful. To apply the variational approach to the localized BEC, we adopt the following variational ansatz

$$u(x, t) = \frac{1}{\pi^{1/4}} \sqrt{\frac{N}{w}} \exp \left[-\frac{(x - x_0)^2}{2w^2} \right] \times \exp \{ i [\gamma(x - x_0) + \beta(x - x_0)^2 + \phi] \}, \quad (4)$$

with w the spatial width of the localized state centered at x_0 , γ the linear phase coefficient, β the chirp and ϕ the phase. These are time-dependent parameters [30]. The Lagrangian of the system is [31, 32]

$$\begin{aligned} L(t) &= \int_{-\infty}^{\infty} \left[\frac{i}{2} \left(u^* \frac{\partial u}{\partial t} - u \frac{\partial u^*}{\partial t} \right) - \frac{1}{2} \left| \frac{\partial u}{\partial x} \right|^2 \right. \\ &\quad \left. - \frac{1}{2} g(x) |u|^4 - V(x) |u|^2 \right] dx \\ &= N(\gamma \dot{x}_0 - \frac{1}{2} \dot{\beta} w^2 - \dot{\phi}) - \frac{N}{2} \left(\frac{1}{2w^2} + \gamma^2 + 2\beta^2 w^2 \right) \\ &\quad + N^2 L_M + N L_V, \end{aligned} \quad (5)$$

where the overhead dot denotes time derivative, the star denotes complex conjugation and

$$L_M = \frac{\varepsilon}{4\sqrt{2}\pi w} \sum_{l=1}^2 A_l \left[\cos(2k_l x_0) \exp \left(-\frac{k_l^2 w^2}{2} \right) - 1 \right], \quad (6)$$

$$L_V = -\frac{1}{2} \sum_{l=1}^2 A_l [1 - \cos(2k_l x_0) \exp(-k_l^2 w^2)]. \quad (7)$$

We use the variational Euler-Lagrange equation

$$\frac{\partial L}{\partial \sigma} - \frac{d}{dt} \frac{\partial L}{\partial \dot{\sigma}} = 0, \quad (8)$$

where the variational parameters are $\sigma = \phi, x_0, \gamma, \beta$, and w . The first variational equation using $\sigma = \phi$ yields $N = \text{constant}$. We take this constant to be unity and use it in the subsequent equations. The other choices of σ respectively, lead to the following equations

$$\dot{\gamma} = -\frac{\varepsilon}{2\sqrt{2\pi}w} \sum_{l=1}^2 A_l k_l \sin(2k_l x_0) \exp\left(-\frac{1}{2}k_l^2 w^2\right) - \sum_{l=1}^2 A_l k_l \sin(2k_l x_0) \exp(-k_l^2 w^2), \quad (9)$$

$$\dot{x}_0 = \gamma, \quad (10)$$

$$\dot{w} = 2\beta w \equiv F(w, \beta), \quad (11)$$

$$\dot{\beta} = \frac{1}{2w^4} - 2\beta^2 + \frac{1}{w} \frac{\partial L_M}{\partial w} + \frac{1}{w} \frac{\partial L_V}{\partial w} \equiv G(w, \beta). \quad (12)$$

The Hamiltonian of the BEC is

$$H = \dot{x}_0 \frac{\partial L}{\partial \dot{x}_0} + \dot{\phi} \frac{\partial L}{\partial \dot{\phi}} + \dot{\beta} \frac{\partial L}{\partial \dot{\beta}} - L = \frac{1}{2} \left(\frac{1}{2w^2} + \gamma^2 + 2\beta^2 w^2 \right) - L_M - L_V. \quad (13)$$

Equations (11) and (12) determine the evolution of the width w once x_0 is known. Equations (9) and (10) determine the evolution of center x_0 once the width w is known. To study the dynamics of the localized state, we insert Eq. (9) into Eq. (10) to get an anharmonic effective potential V_{eff} :

$$\frac{d^2 x_0}{dt^2} = -\frac{\partial V_{\text{eff}}}{\partial x_0} \equiv -\frac{\partial}{\partial x_0} (V_{\text{effM}} + V_{\text{effV}}), \quad (14)$$

$$V_{\text{effM}} = \frac{-\varepsilon}{4\sqrt{2\pi}w} \sum_{l=1}^2 A_l \cos(2k_l x_0) \exp\left(-\frac{k_l^2 w^2}{2}\right), \quad (15)$$

$$V_{\text{effV}} = -\frac{1}{2} \sum_{l=1}^2 A_l \cos(2k_l x_0) \exp(-k_l^2 w^2). \quad (16)$$

The effective potential has two terms. The second term on the right of Eq. (14), V_{effV} , arises from the bichromatic OL and contributes to an attractive well, if $|x_0|$ is small enough. The first term, V_{effM} , is induced by the spatial modulation of the nonlinearity and is actually a pseudo-potential [33]. The pseudo potential is quasi periodic and is a potential barrier or well depending on the sign and value of the coefficient ε .

III. STATIONARY LOCALIZED STATE

The stationary states are obtained by setting the time derivative in Eqs. (9) – (12) to zero. Then the simplest solution of Eqs. (9) and (10) is $x_0 = 0$ and we consider below an immobile localized state at origin ($x_0 = 0$) with

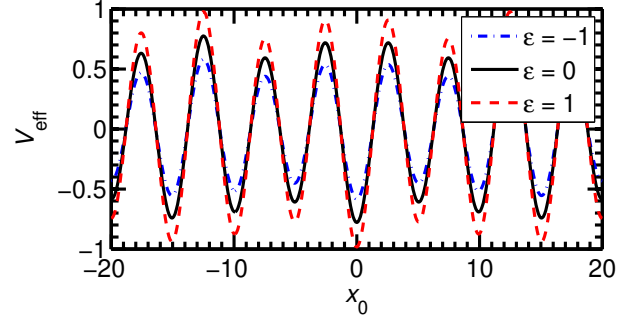


FIG. 1: (Color online) The dimensionless effective potentials V_{eff} “felt” by an immobile localized state for different ε from Eqs. (15) and (16) where the width w is calculated from Eq. (18).

$\gamma = 0$. Equations (11) and (12) determine w and can be written as

$$\beta_0 = 0, \quad (17)$$

$$1 + \frac{\varepsilon w_0}{2\sqrt{2\pi}} \sum_{l=1}^2 A_l \left[1 - (1 + k_l^2 w_0^2) \exp\left(-\frac{1}{2}k_l^2 w_0^2\right) \right] - 2w_0^4 \sum_{l=1}^2 A_l k_l^2 \exp(-k_l^2 w_0^2) = 0. \quad (18)$$

The effective potential felt by a stationary localized state at $x = x_0 = 0$ is obtained from Eqs. (14) – (16) and is plotted in Fig. 1 where the width w is obtained by solving numerically Eq. (18). With the increase of ε , the strength of both disorder and the quasi periodic effective potential increases.

To understand the effects of the coefficient ε , we obtain the stationary localized states by solving Eq. (1) numerically with real-time Split-step Fourier spectral method with a space step 0.04 and time step 0.0001. We checked the accuracy of the results by varying the space and time steps and the total number of space and time steps. To compare with numerics, the variational width is obtained by solving Eq. (18).

Typical numerical and variational results for density, width and Hamiltonian of the localized state at $x = 0$ are exhibited in Fig. 2 for $-1 \leq \varepsilon \leq 1$. The variational Hamiltonian is obtained from Eq. (13) and the numerical Hamiltonian is obtained from $H = \int_{-\infty}^{\infty} [|u'|^2/2 + g(x)|u|^4/2 + V(x)|u|^2] dx$. Figures 2 (a) and (b) exhibit the density of the stationary localized states corresponding to $\varepsilon = -1$ and 1, respectively. Figures 2 (c) and (d) exhibit the variation of w and H with ε . The numerical width w in Fig. 2 (c) is $\sqrt{2}$ times the root-mean-square (rms) size of the BEC. Figures 2 indicate that the numerical results are in good agreement with the variational results. Figure 2 (c) shows that the width decreases and Fig. 2 (d) shows that the Hamiltonian increases with the change of ε from negative to positive. The dependence

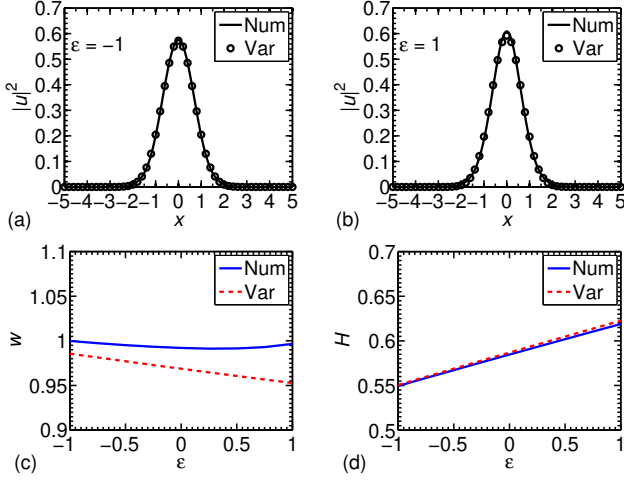


FIG. 2: (Color online) Numerical (lines) and variational (chain of symbols) densities $|u|^2$ of the localized BEC versus x for (a) $\varepsilon = -1$, (b) $\varepsilon = 1$. (c) Numerical (solid lines) and variational (dashed lines) dimensionless widths w versus ε and (d) Hamiltonian versus ε . (All quantities are dimensionless.)

of the variational width on ε can be qualitatively understood as follows. The height of the central well of the effective potential increases with increasing ε as shown in Fig. 1. Hence the central part of the localized state with a Gaussian shape becomes narrow with the increase of ε , as can be seen from Figs. 2 (a) and (b). The variational Gaussian ansatz only represents this central part and hence the variational width decreases with increasing ε . However, the numerical width (rms size) shown in Fig. 2 (c) receives nontrivial contributions from both the central Gaussian part and the extended exponential tail of the wave function (viz. Fig. 4 (a)), making it difficult to predict even qualitatively the variation of the numerical width with ε . It is interesting to compare these results with those of a collisionally homogeneous condensate where a constant negative (attractive) nonlinearity leads to a reduction of the width and a constant positive (repulsive) nonlinearity increases the width of the localized state [15]. The numerical width is larger than the variational width in Fig. 2 (c) due to the long exponential tail of the numerically obtained BEC (viz., Fig. 4). Also, the difference between the variational and numerical widths increases for larger values of ε , because for larger ε the exponential tail is more pronounced resulting in a larger width (viz., Fig. 4).

It is important to investigate the stability of the stationary state governed by Eqs. (17) and (18) against perturbation by a standard linear stability analysis. Introducing small fluctuations around the stationary solution (w_0, β_0) , $w'(t) = w(t) - w_0$, $\beta'(t) = \beta(t) - \beta_0$, and linearizing Eqs. (11) and (12) indicated by them, a set

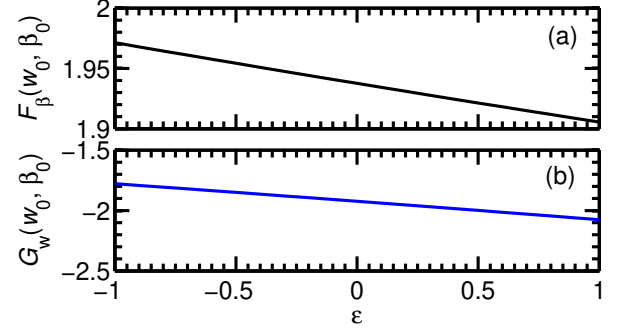


FIG. 3: (Color online) (a) The dimensionless functions $F_\beta(w_0, \beta_0)$ and (b) $G_w(w_0, \beta_0)$ versus ε . It shows that the signs of the two functions are opposite for $-1 \leq \varepsilon \leq 1$.

of two linear equations are obtained:

$$\frac{dw'(t)}{dt} = F_w(w_0, \beta_0)w'(t) + F_\beta(w_0, \beta_0)\beta'(t), \quad (19)$$

$$\frac{d\beta'(t)}{dt} = G_w(w_0, \beta_0)w'(t) + G_\beta(w_0, \beta_0)\beta'(t), \quad (20)$$

where the subscripts w and β denote a derivative with respect to the respective variable. Assuming the solution of $w'(t)$ and $\beta'(t)$ in exponential form, $\sim \exp(\mathcal{E}t)$, the eigen value \mathcal{E} is

$$2\mathcal{E} = F_w(w_0, \beta_0) + G_\beta(w_0, \beta_0) \pm \left\{ [F_w(w_0, \beta_0) + G_\beta(w_0, \beta_0)]^2 + 4F_\beta(w_0, \beta_0)G_w(w_0, \beta_0) \right\}^{1/2}. \quad (21)$$

From Eqs. (11) and (12), we find $F_w(w_0, \beta_0) = 0$, $G_\beta(w_0, \beta_0) = 0$, and

$$F_\beta(w_0, \beta_0) = 2w_0, \quad (22)$$

$$G_w(w_0, \beta_0) = -\frac{2}{w_0^5} + 2w_0 \sum_{l=1}^2 A_l k_l^4 \exp(-k_l^2 w_0^2) + \frac{\varepsilon}{4\sqrt{2\pi}w_0^4} \sum_{l=1}^2 A_l \left[-3 + (3 + 2k_l^2 w_0^2 + k_l^4 w_0^4) \times \exp\left(-\frac{1}{2}k_l^2 w_0^2\right) \right], \quad (23)$$

which leads to the eigen-values

$$\mathcal{E} = \pm [F_\beta(w_0, \beta_0)G_w(w_0, \beta_0)]^{1/2}. \quad (24)$$

To investigate the stability, Eq. (18) is first solved to get w_0 as a function of ε . This result is then inserted in Eqs. (22) and (23) to get $F_\beta(w_0, \beta_0)$ and $G_w(w_0, \beta_0)$. The graphical representation of the two functions is shown in Figs. 3 (a) and (b). In the case of a small coefficient ε , we can find that $G_w(w_0, \beta_0) < 0$ and $F_\beta(w_0, \beta_0) = 2w_0 >$

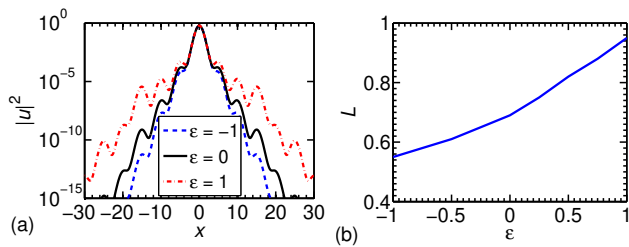


FIG. 4: (Color online) (a) The numerically obtained dimensionless density $|u|^2$ versus dimensionless x for different ϵ . (b) The dimensionless localization lengths L versus ϵ . The localization length L is obtained by exponential fitting to the tails of density distribution with $\sim \exp(-|x|/L)$

0. Thus, both the eigen-values from Eq. (24) must be imaginary, and the localized state from Eqs. (17) and (18) is stable against small perturbation.

Anderson localization in a weakly disordered potential is characterized by a long exponential tail of the localized state. For collisionally homogeneous condensates, the experimental [5] and theoretical [15] investigations have demonstrated that the localized BECs have an exponential tail for weakly-interacting or non-interacting BEC in a quasi-periodic OL. In order to observe the effect of spatially modulated nonlinearity on the tail region, we plot in Fig. 4 (a) the density distribution $|u|^2$ of the stationary BEC on log scale. As we see, the long exponential tail extends from $x \approx \pm 2$ to $x \approx \pm 20$, whereas the central part of density for $|x| < 2$ represents a Gaussian distribution. By an exponential fitting of the exponential function $\sim \exp(-|x|/L)$ to the tails of density distribution, the localization length L versus ϵ is illustrated in Fig. 4 (b) which shows that L increases nonlinearly with ϵ . An increase in ϵ represents a decrease in disorder thus resulting in larger values of localization length.

IV. DYNAMICS OF LOCALIZED STATE

To get further insight into the effects of the spatially modulated nonlinearity ϵ on the localized states, we now study some dynamics of the localized state. First, we study numerically the oscillation of the localized states in an external potential. According to Eqs. (14) - (16), the motion of the localized BEC can be approximately regarded as that of a particle inside an effective potential V_{eff} . Because of the exponential tail and elasticity of the localized state, although the variational results may not be good for the dynamical evolution, they can provide a qualitative physical understanding of the dynamics using the effective potential. To study the motion of the localized state, first we create a stationary localized BEC with spatially modulated nonlinearity in the bichromatic OL. Successively, at $t = 0$, we suddenly introduce an initial momentum $p_0 = 0.1$ by $u(x) \rightarrow u_0(x) \exp(ip_0 x)$, where u_0 is the wave function of the stationary localized BEC.

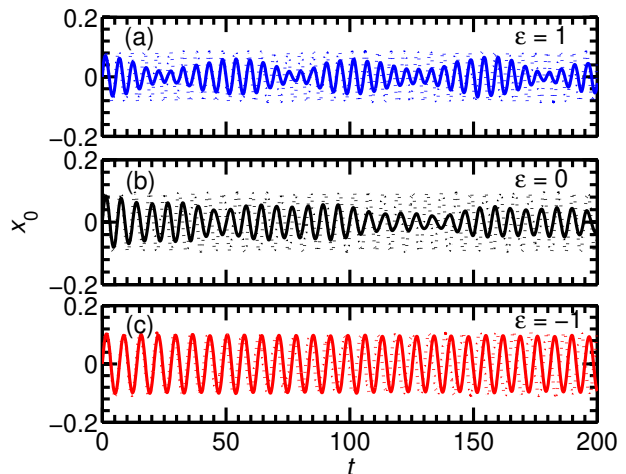


FIG. 5: (Color online) The center of the localized state x_0 versus time t (both dimensionless) during the location oscillation initiated by suddenly introducing an initial momentum $p_0 = 0.1$ by the transformation $u \rightarrow u_0 \exp(ip_0 x)$ for $\epsilon =$ (a) 1, (b) 0, and (c) -1 : numerical result (full line) and variational result (dotted line).

From the experimental point of view, the initial momentum can be given by suddenly moving the OL [34]. It is found that after the perturbation, the density envelope suffers an abrupt change but remains localized. Actually, the localized BEC is an elastic object and not a rigid one. Hence, both the center and the density distribution of the localized state perform oscillations.

The evolution of the center x_0 of the localized BEC as obtained from numerical simulation (full line) is shown in Fig. 5 where x_0 is obtained by instant Gaussian-function fitting to the central region of the density distribution. The variational results are also shown in this figure. The top, middle and bottom panels correspond to $\epsilon = 1, 0$, and -1 , respectively. We find that, in general, the oscillation of the localized state could be quasi periodic after an initial damping, which can be explained on the basis of energy conservation. Because of the deformation of the density envelope, a part of the initial kinetic energy is converted into elastic energy of deformation and this leads to the damped oscillation. This deformation will be larger for large ϵ ($= 1$), when the localized state is loosely bound with large exponential tail (viz. Fig. 4 (a)). Consequently, an oscillation of the center x_0 with rapidly varying amplitude is found denoting easy periodic transfer of energy between location oscillation and deformation. For small ϵ ($= -1$), the localized state is more compact and tightly bound, so that it can be treated like a rigid object. The exchange of energy is less probable in that case, and a periodic oscillation of the center x_0 with constant amplitude is found. Eventually, the energy of deformation is liberated leading to an increase in the amplitude of oscillation. During the subsequent oscillation cycle, the conversion between the kinetic energy and elas-

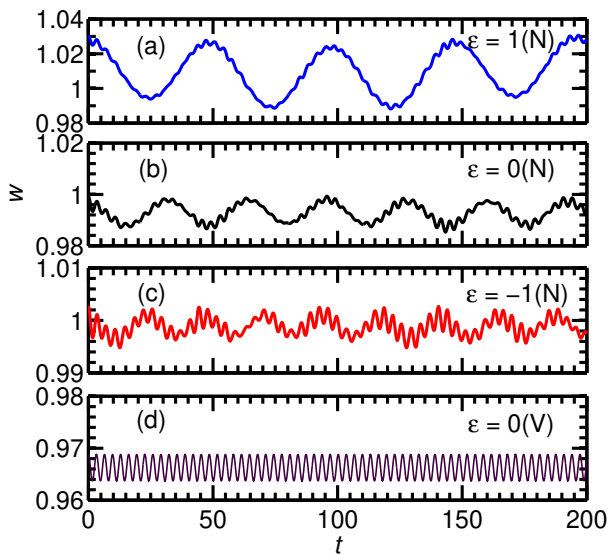


FIG. 6: (Color online) Numerical (N) result for dimensionless pulse width w of the localized state versus dimensionless time t during breathing oscillation initiated by suddenly changing the strength of the secondary lattice s_2 from 3 to 3.5 for $\varepsilon =$ (a) 1, (b) 0, and (c) -1 . We also show the variational result (V) of pulse width w from a solution of Eqs. (11) and (12) with condition $w(t=0) = 0.9688$ and $\beta(t=0) = 0$.

tic strain energy causes the quasi-periodical movement of the localized state. In the variational formulation the exchange of kinetic energy to the energy of deformation is not allowed and the resultant oscillation is of a fixed amplitude without damping. Nevertheless, the numerical frequency of location oscillation is in agreement with the variational frequency within an estimated error of about 2.5%. As pointed out in Sec. III, a positive ε leads to a tighter trapping and vice versa. Then, with the same initial velocity, the tighter trapping causes the localized state to oscillate with larger frequency and smaller amplitude, and a weaker trapping leads to a smaller frequency and larger amplitude of oscillation as indicated in the numerical results of Fig. 5. The variational frequency follows the same trend as ε is changed from positive values to negative values.

Next we consider a breathing oscillation of the localized BEC, started by suddenly changing the strength of the secondary lattice s_2 from 3 to 3.5 at $t = 0$. We investigate how the breathing oscillation of the localized BEC is changed by the spatially modulated nonlinearity. Then, the nonlinearity in Eq. (1), $g(x)$, also changes with the new OL potential. We present numerical results in Fig. 6 (a), (b), and (c) for the time evolution of the width w of the localized state for $\varepsilon = 1, 0$ and -1 , respectively. The variational equations (11) and (12) were

solved to obtain the oscillation of the central part and this result is shown in Fig. 6 (d) for $\varepsilon = 0$. (The Gaussian variational ansatz without any exponential tail only carries information about the central part.) There are two regions of the localized state which oscillate with two distinct frequencies: (i) the central region with Gaussian distribution and (ii) the outer tail with exponential distribution. The net result is the harmonic oscillation of the width with a small frequency and large amplitude due to the oscillation of the exponential tail, which is modulated by rapid oscillation coming from the central Gaussian part. The variational frequency as obtained from Fig. 6 (d) is found to be identical with the frequency of modulation of the numerical width, which confirms that the modulation in Figs. 6 (a), (b) and (c) is coming from the oscillation of the central part of the condensate. The renewed oscillation in Figs. 5 and 6 confirms the stability of the stationary localized BECs.

V. SUMMARY

In this paper, using the numerical and variational solution of the time-dependent GP equation, we studied the stationary and dynamic characteristics of a cigar-shaped localized BEC with spatially inhomogeneous nonlinearity in a bichromatic quasi-periodic 1D OL potential. This investigation reveals that the spatially inhomogeneous nonlinearity produces a pseudo-potential which changes the strength of the disorder and the height of the quasi periodic effective potential felt by the localized BEC. With a larger spatially modulated coefficient ε , the localization length and Hamiltonian will be larger.

We also study the stability of the stationary localized state using the linear stability analysis and find it is dynamically stable under small perturbations. The stability is also verified by numerical simulation. In respect to dynamics, we investigate the location oscillation (oscillation of the center) and breathing oscillation of the localized BEC, and find that both oscillations are quasi periodic because of the quasi periodic effective potential. The frequency of quasi periodic oscillations of the center of the BEC increases as ε increases. For the breathing oscillations, the two exponential tails also are symmetric around the center at $x = 0$. The present study is useful for an understanding of the statics and dynamics of Anderson localization and for planning new experiments with collisionally inhomogeneous BEC.

Acknowledgments

FAPESP (Brazil) and CNPq (Brazil) provided partial support.

-
- [1] P. W. Anderson, Phys. Rev. **109**, 1492 (1958).
- [2] D. S. Wiersma, P. Bartolini, Ad Lagendijk *et al.*, Nature (London) **390**, 671 (1997); F. Scheffold, R. Lenke, R. Tweer *et al.*, *ibid.* **398**, 206 (1999); R. Dalichaouch, J. P. Armstrong, S. Schultz *et al.*, *ibid.* **354**, 53 (1991); A. A. Chabanov, M. Stoytchev, A. Z. Genack *et al.*, *ibid.* **404**, 850 (2000).
- [3] R. L. Weaver, Wave Motion **12**, 129 (1990).
- [4] J. Billy, V. Josse, Z. Zuo, *et al.*, Nature (London) **453**, 891 (2008).
- [5] G. Roati, C. D'Errico, L. Fallani, *et al.*, Nature (London) **453**, 895 (2008).
- [6] L. Fallani, C. Fort and M. Inguscio, Adv. At. Mol. Opt. Phys. **56**, 119 (2008); J. E. Lye, L. Fallani, M. Modugno, *et al.*, Phys. Rev. Lett. **95**, 070401 (2005).
- [7] L. Fallani, J. E. Lye, V. Guarrera, C. Fort, and M. Inguscio, Phys. Rev. Lett. **98**, 130404 (2007).
- [8] P. G. Harper, Proc. Phys. Soc. London Sect. A **68**, 874 (1955).
- [9] S. Aubry and G. André, Ann. Israel. Phys. Soc. **3**, 33 (1980).
- [10] L. Sanchez-Palencia, D. Clément, P. Lugan, *et al.*, Phys. Rev. Lett. **98**, 210401 (2007); D. Clément, A. F. Varón, M. Hugbart, *et al.*, *ibid.* **95**, 170409 (2005); T. Paul, M. Albert, P. Schlagheck, P. Leboeuf, and N. Pavloff, Phys. Rev. A **80**, 033615 (2009); T. Paul, P. Schlagheck, P. Leboeuf, and N. Pavloff, Phys. Rev. Lett. **98**, 210602 (2007).
- [11] G. Roux, T. Barthel, I. P. McCulloch, *et al.*, Phys. Rev. A **78**, 023628 (2008); B. Damski, J. Zakrzewski, L. Santos, P. Zoller, and M. Lewenstein, Phys. Rev. Lett. **91**, 080403 (2003); T. Schulte, S. Drenkelforth, J. Kruse, *et al.*, *ibid.* **95**, 170411 (2005); T. Roscilde, Phys. Rev. A **77**, 063605 (2008); X. Deng, R. Citro, E. Orignac, *et al.*, Eur. Phys. J. B **68**, 435 (2009).
- [12] J. Chabé, G. Lemarié, B. Grémaud, *et al.*, Phys. Rev. Lett. **101**, 255702 (2008); E. E. Edwards, M. Beeler, T. Hong, and S. L. Rolston, Phys. Rev. Lett. **101**, 260402 (2008).
- [13] R. C. Kuhn, C. Miniatura, D. Delande, O. Sigwarth, and C. A. Muller, Phys. Rev. Lett. **95**, 250403 (2005); S. E. Skipetrov, A. Minguzzi, B. A. vanTiggelen, and B. Shapiro, Phys. Rev. Lett. **100**, 165301 (2008); E. Abrahams, P. W. Anderson, D. C. Licciardello, and T. V. Ramakrishnan, Phys. Rev. Lett. **42**, 673 (1979).
- [14] A. S. Pikovsky and D. L. Shepelyansky, Phys. Rev. Lett. **100**, 094101 (2008); S. Flach, D. O. Krimer, and Ch. Skokos, Phys. Rev. Lett. **102**, 024101 (2009); I. García-Mata and D. L. Shepelyansky, Phys. Rev. E **79**, 026205 (2009); Ch. Skokos, D. O. Krimer, S. Komineas, and S. Flach, Phys. Rev. E **79**, 056211 (2009); P. Lugan, D. Clement, P. Bouyer, A. Aspect, and L. Sanchez-Palencia, Phys. Rev. Lett. **99**, 180402 (2007); J. E. Lye, L. Fallani, C. Fort, *et al.*, Phys. Rev. A **75**, 061603(R) (2007).
- [15] S. K. Adhikari and L. Salasnich, Phys. Rev. A **80**, 023606 (2009); Y. Cheng and S. K. Adhikari, Phys. Rev. A **81**, 023620 (2010); Y. Cheng and S. K. Adhikari, Phys. Rev. A **82**, 013631 (2010); Y. Cheng and S. K. Adhikari, Laser Phys. Lett. **7**, 824 (2010); S. K. Adhikari, Phys. Rev. A **81**, 043636 (2010).
- [16] S. Inouye, M. R. Andrews, J. Stenger, *et al.*, Nature (London) **392**, 151 (1998).
- [17] M. Theis, G. Thalhammer, K. Winkler, *et al.*, Phys. Rev. Lett. **93**, 123001 (2004).
- [18] G. Roati, M. Zaccanti, C. D'Errico, *et al.*, Phys. Rev. Lett. **99**, 010403 (2007); P. Zhang, P. Naidon, and M. Ueda, Phys. Rev. Lett. **103**, 133202 (2009).
- [19] P. O. Fedichev, Yu. Kagan, G. V. Shlyapnikov, and J. T. M. Walraven, Phys. Rev. Lett. **77**, 2913 (1996).
- [20] H. Sakaguchi and B. A. Malomed, Phys. Rev. E **72**, 046610 (2005).
- [21] J. Belmonte-Beitia, V. M. Pérez-García, V. Vekslerchik, and V. V. Konotop, Phys. Rev. Lett. **100**, 164102 (2008); A. T. Avelar, D. Bazeia, and W. B. Cardoso, Phys. Rev. E **79**, 025602(R) (2009); J. Belmonte-Beitia and J. Cuevas, J. Phys. A **42**, 165201 (2009).
- [22] F. Kh. Abdullaev, R. M. Galimzyanov, M. Brtko, and L. Tomio, Phys. Rev. E **79**, 056220 (2009); F. Kh. Abdullaev, A. Gammal, M. Salerno, and L. Tomio, Phys. Rev. A **77**, 023615 (2008); F. Abdullaev, A. Gammal and L. Tomio, J. Phys. B **37**, 635 (2004).
- [23] R. Yamazaki, S. Taie, S. Sugawa, and Y. Takahashi, Phys. Rev. Lett. **105**, 050405 (2010).
- [24] P. Niarchou, G. Theocharis, P. G. Kevrekidis, P. Schmelcher, and D. J. Frantzeskakis, Phys. Rev. A **76**, 023615 (2007); G. Theocharis, P. Schmelcher, P. G. Kevrekidis, and D. J. Frantzeskakis, Phys. Rev. A **72**, 033614 (2005); A. S. Rodrigues, P. G. Kevrekidis, M. A. Porter, *et al.*, Phys. Rev. A **78**, 013611 (2008); V. M. Pérez-García and R. Pardo, Physica D **238**, 1352 (2009).
- [25] G. Theocharis, P. Schmelcher, P. G. Kevrekidis, and D. J. Frantzeskakis, Phys. Rev. A **74**, 053614 (2006); J. Garnier and F. Kh. Abdullaev, Phys. Rev. A **74**, 013604 (2006); F. Kh. Abdullaev, A. Gammal, H. L. F. da Luz, and L. Tomio, Phys. Rev. A **76**, 043611 (2007).
- [26] F. Abdullaev, A. Abdumalikov, and R. Galimzyanov, Phys. Lett. A **367**, 149 (2007).
- [27] C. A. G. Buitrago and S. K. Adhikari, J. Phys. B **42**, 215306 (2009); L. Salasnich, A. Parola, and L. Reatto, Phys. Rev. A **65**, 043614 (2002); S. K. Adhikari and B. A. Malomed, Phys. Rev. A **79**, 015602 (2009); Y. Cheng, J. Phys. B **42**, 205005 (2009); P. Muruganandam and S. K. Adhikari, Comput. Phys. Commun. **180**, 1888 (2009).
- [28] P. J. Y. Louis, E. A. Ostrovskaya, C. M. Savage, and Y. S. Kivshar, Phys. Rev. A **67**, 013602 (2003).
- [29] M. Modugno, New J. Phys. **11**, 033023 (2009); M. Larcher, F. Dalfovo, and M. Modugno, Phys. Rev. A **80**, 053606 (2009).
- [30] R. Scharf and A. R. Bishop, Phys. Rev. E **47**, 1375 (1993).
- [31] V. M. Pérez-García, H. Michinel, J. I. Cirac, M. Lewenstein, and P. Zoller, Phys. Rev. A **56**, 1424 (1997).
- [32] Y. Cheng, R. Gong, and H. Li, Optics Exp. **14**, 3594 (2006).
- [33] T. Mayteevarunyoo, B. A. Malomed, and G. Dong, Phys. Rev. A **78**, 053601 (2008).
- [34] J. Mun *et al.*, Phys. Rev. Lett. **99**, 150604 (2007).